INFRASOUND SIGNAL CHARACTERISTICS FROM SMALL EARTHQUAKES

Stephen J. Arrowsmith[1], J. Mark Hale[2], Relu Burlacu[2], Kristine L. Pankow[2], Brian W. Stump[3], Chris Hayward[3], George E. Randall[1], and Steven R. Taylor[4]

Los Alamos National Laboratory[1], University of Utah[2], Southern Methodist University[3], and Rocky Mountain Geophysics[4]

Sponsored by the National Nuclear Security Administration

Award No. DE-AR52-09NA29325
Proposal No. BAA09-49

ABSTRACT

Physical insight into source properties that contribute to the generation of infrasound signals is critical to understanding the differences in atmospheric signals from near-surface explosions and earthquakes. This understanding provides the background for assessing the possibility of signal discrimination from these different source types. This research attempts to develop a dataset necessary to address these issues and to provide constraints to the development of a physical basis for signal generation. The data component of this study is supported by the operation and maintenance of nine infrasonic arrays by the University of Utah Seismograph Stations (UUSS). Each array consists of four elements with an aperture of ~150 m, with one element being co-located with a seismic station. One of the goals of this project is the recording of infrasound from earthquakes of moderate size on multiple infrasound arrays in order to assess the location of the infrasound source and its sensitivity to source mechanism and depth, as well as the characteristics of the signal. We report on processing results using infrasound data for all $M_L > 3$ earthquakes in the UUSS catalog from January 1, 2007, through March 31, 2011. We then focus on multi-array recordings of infrasound data from a moderate-sized event (M_w 4.6) in Utah. This event occurred on January 3, 2011, at 12:06:37 UTC, within a known seismically active belt along the western side of the Sevier Valley in the Tushar Mountains (in the proximity of the city of Circleville). The event was widely felt in the surrounding communities, had a normal faulting mechanism and a depth constrained, by full moment tensor estimation, between 5 and 9 km. The main shock and 85 aftershocks were recorded by Utah's regional seismic network. Epicentral infrasound from the main event was detected by six of the nine infrasonic arrays distributed throughout Utah. The event allows us to explore (as part of the on-going project) possible models of infrasound generation from earthquakes based on models of earthquake source ground motion parameters (acceleration, velocity). We report on preliminary modeling of the Circleville earthquake. We use a three-dimensional (3D) finite difference technique to model acceleration time histories on a two-dimensional (2D) grid in the epicenter region. These accelerations, scaled by peak acceleration estimates from ShakeMap, provide the initial conditions for modeling the near-field acoustic pressure waveform using the Rayleigh integral. This source term provides the initial conditions for time domain parabolic equation modeling, which predicts the acoustic waveform at the receiver. Our preliminary modeling results demonstrate that the infrasound recorded from the Circleville earthquake at the six arrays is consistent with a "baffled piston" model for the generation of infrasound from earthquakes.

Report Documentation Page

Form Approved
OMB No. 0704-0188

1. REPORT DATE	2. REPORT TYPE	3. DATES COVERED
SEP 2011		**00-00-2011 to 00-00-2011**

4. TITLE AND SUBTITLE	5a. CONTRACT NUMBER
Infrasound Signal Characteristics from Small Earthquakes	5b. GRANT NUMBER
	5c. PROGRAM ELEMENT NUMBER
6. AUTHOR(S)	5d. PROJECT NUMBER
	5e. TASK NUMBER
	5f. WORK UNIT NUMBER
7. PERFORMING ORGANIZATION NAME(S) AND ADDRESS(ES) **Los Alamos National Laboratory,P.O. Box 1663 ,Los Alamos,NM,87545**	8. PERFORMING ORGANIZATION REPORT NUMBER
9. SPONSORING/MONITORING AGENCY NAME(S) AND ADDRESS(ES)	10. SPONSOR/MONITOR'S ACRONYM(S)
	11. SPONSOR/MONITOR'S REPORT NUMBER(S)

12. DISTRIBUTION/AVAILABILITY STATEMENT
Approved for public release; distribution unlimited

13. SUPPLEMENTARY NOTES
Published in the Proceedings of the 2011 Monitoring Research Review - Ground-Based Nuclear Explosion Monitoring Technologies, 13-15 September 2011, Tucson, AZ. Volume II. Sponsored by the Air Force Research Laboratory (AFRL) and the National Nuclear Security Administration (NNSA). U.S. Government or Federal Rights License

14. ABSTRACT

Physical insight into source properties that contribute to the generation of infrasound signals is critical to understanding the differences in atmospheric signals from near-surface explosions and earthquakes. This understanding provides the background for assessing the possibility of signal discrimination from these different source types. This research attempts to develop a dataset necessary to address these issues and to provide constraints to the development of a physical basis for signal generation. The data component of this study is supported by the operation and maintenance of nine infrasonic arrays by the University of Utah Seismograph Stations (UUSS). Each array consists of four elements with an aperture of ~150 m, with one element being co-located with a seismic station. One of the goals of this project is the recording of infrasound from earthquakes of moderate size on multiple infrasound arrays in order to assess the location of the infrasound source and its sensitivity to source mechanism and depth, as well as the characteristics of the signal. We report on processing results using infrasound data for all ML > 3 earthquakes in the UUSS catalog from January 1, 2007, through March 31, 2011. We then focus on multiarray recordings of infrasound data from a moderate-sized event (Mw 4.6) in Utah. This event occurred on January 3 2011, at 12:06:37 UTC, within a known seismically active belt along the western side of the Sevier Valley in the Tushar Mountains (in the proximity of the city of Circleville). The event was widely felt in the surrounding communities, had a normal faulting mechanism and a depth constrained, by full moment tensor estimation, between 5 and 9 km. The main shock and 85 aftershocks were recorded by Utah?s regional seismic network. Epicentral infrasound from the main event was detected by six of the nine infrasonic arrays distributed throughout Utah. The event allows us to explore (as part of the on-going project) possible models of infrasound generation from earthquakes based on models of earthquake source ground motion parameters (acceleration, velocity). We report on preliminary modeling of the Circleville earthquake. We use a three-dimensional (3D) finite difference technique to model acceleration time histories on a two-dimensional (2D) grid in the epicenter region. These accelerations, scaled by peak acceleration estimates from ShakeMap, provide the initial conditions for modeling the near-field acoustic pressure waveform using the Rayleigh integral. This source term provides the initial conditions for time domain parabolic equation modeling, which predicts the acoustic waveform at the receiver. Our preliminary modeling results demonstrate that the infrasound recorded from the Circleville earthquake at the six arrays is consistent with a ?baffled piston? model for the generation of infrasound from earthquakes.

15. SUBJECT TERMS

16. SECURITY CLASSIFICATION OF:			17. LIMITATION OF ABSTRACT	18. NUMBER OF PAGES	19a. NAME OF RESPONSIBLE PERSON
a. REPORT	b. ABSTRACT	c. THIS PAGE			
unclassified	**unclassified**	**unclassified**	**Same as Report (SAR)**	**12**	

OBJECTIVES

A wide range of natural and man-made source types generate seismo-acoustic signals. The analysis of both the seismic and infrasound signals accompanying these sources provides an opportunity for characterizing them, especially for those that occur near the solid earth/atmosphere boundary. Extensive research has previously been undertaken on the generation of infrasound from surface explosions (Sorrells et al., 1997; Che et al., 2002; and McKenna et al., 2007) with the work identifying the importance of path-dependent atmospheric effects in the analysis (Arrowsmith et al., 2008). Most previous studies on infrasound from earthquakes have focused on medium to large earthquakes recorded at distances greater than 220 km (e.g., Kim et al., 2004; Mutschlecner and Whitaker, 2005; and Le Pichon et al., 2006).

The primary objective of this work is to acquire seismo-acoustic data in a network setting in order to determine whether small earthquakes generate infrasound. Multiple seismo-acoustic arrays are necessary in order to assess the impact of propagation path effects on the observations. Further, the work is intended to provide a basis for modeling the infrasound signals with constrained earthquake source parameters such as depth, source mechanism, and local strong ground motions. Studies of medium to large earthquakes suggest a linear relationship between earthquake magnitude ($M_L > 4$) and the duration of stratospheric returns and between magnitude and the log of the amplitude of wind-corrected stratospheric returns scaled to a reference distance (Mutschlecner and Whitaker, 2005 and Le Pichon et al., 2006). A second objective is to assess these empirical relationships for small earthquakes.

The first step in reaching the objectives of this study has been the design, installation, and operation of a network of seismo-acoustic arrays co-located with seismic stations operated by the UUSS. The new arrays are in the state of Utah within ~115 km of the axis of the Intermountain Seismic Belt (Smith and Arabasz, 1991), a zone of seismicity that extends from Nevada and Arizona northeast to Montana. In addition to the seismicity, the region is marked by complex topography, open-pit quarries, and subsurface coal mining, resulting in a diverse set of sources capable of generating seismo-acoustic signals. Work on this first step has been previously reported (Hale et al., 2010).

The second step in this study has been the acquisition of seismo-acoustic data to extend the magnitude scaling analysis noted earlier to earthquakes with $M_L < 4.0$. New results quantifying the preliminary application of our network data to this problem are included.

The final step in this project is the analysis of source characteristics and earthquake ground motions for earthquakes generating infrasound. With the identification of small earthquakes that generate infrasound, the seismic source characteristics will be used to both interpret the infrasound signals and provide constraints on development of a theoretical model for the generation of earthquake infrasound. The Circleville, Utah, earthquake (M_w 4.6) that occurred on January 3, 2011, provides data for this analysis. Modeling of this event is included.

RESEARCH ACCOMPLISHED

Summary of Seismo-Acoustic Network

Building upon more than four decades of seismic station infrastructure, maintenance, and technical expertise, nine real-time telemetered infrasonic arrays (Figure 1) have been integrated into the regional seismic network in Utah for continuous data recording (Burlacu et al., 2010). Emphasizing cost effectiveness, the integration allows for (1) sharing existing seismic data telemetry solutions and data acquisition capabilities; (2) exchanging infrasonic data with partners, using an established operational system based on Earthworm software (import/export modules); and (3) archiving the infrasonic data at the Incorporated IRIS DMC, using Earthworm waveservers dedicated to both seismic and acoustic data.

Each infrasonic array, with an aperture of ~150 m, consists of four sensors with one of the elements co-located with a seismic sensor that is part of the Utah regional seismic network. Co-locating acoustic and seismic sensors was part of the design plan to characterize and understand problems related to seismic-to-acoustic and acoustic-to-seismic energy coupling. The arrays are equipped with microphones (Chaparral 2, Chaparral 2.5, or IML ST), each fitted with 8 or 10 hoses, for noise reduction. Data recorders (REFTEK 130, Quanterra Q330) are used to digitize data at 100 sps. The microphones are provided by SMU, and the data recorders are from SMU and PASSCAL. PASSCAL also supplied solar panels and cell modems for telemetry.

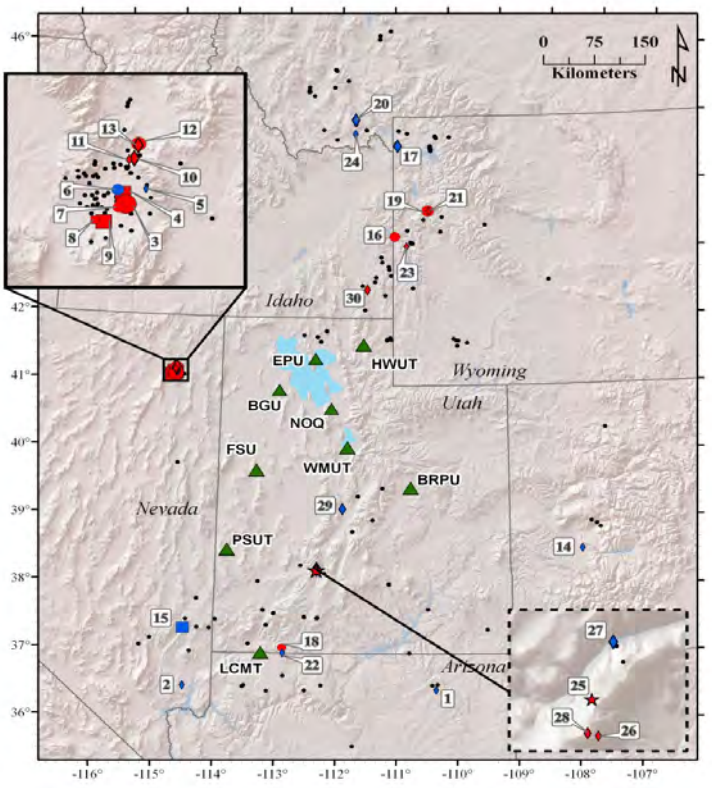

Figure 1. This map illustrates the current configuration of the seismo-acoustic network in Utah (green triangles are infrasound arrays, each with one element co-located with a seismometer). Numbers from 1 to 30 on the map represent event numbers in Table 1 for which infrasound detections with correlation coefficients ≥ 0.5 were recorded. Red symbols represent events for which the backazimuth deviation from the epicenter is ≤ 8°; blue symbols represent events for which the backazimuth deviation is > 8° and ≤ 20°. The number of arrays recording each earthquake varied: diamonds represent detections at a single array, circles at two arrays, squares at three arrays, and the star at six arrays. Symbols are scaled by magnitude. Small black dots are M_L ≥ 3 earthquakes without observed detections. Insets show enlarged areas for the 2008 Wells and 2011 Circleville earthquake sequences.

Comprehensive Search for all M_L > 3 Earthquakes

Available infrasound data from the arrays located in Utah for all M_L > 3 earthquakes (N = 258) in the UUSS earthquake catalog (http://www.quake.utah.edu/EQCENTER/LISTINGS/utahregion.htm) from January 1, 2007, through March 31, 2011, were processed using InfraMonitor (Arrowsmith et al., 2008). When correlating array components, InfraMonitor uses an adaptive noise hypothesis in order to account for time-varying coherent noise sources. Data were filtered between 1 and 5 Hz using a 4th order Butterworth filter. A 20-sec window length with 50% overlap was used in the array processing. Detections were determined using the F-statistic with a 99% confidence interval that the correlation is a signal. For this analysis only detections found in the time window corresponding to atmospheric velocities between 220 and 350 m/s were counted. One detection list includes all events with infrasound observations that produced backazimuth deviations from the epicenter of ≤8° and correlation coefficients ≥ 0.5. A second detection list includes all events with infrasound backazimuth deviations >8° and ≤20° and correlation coefficients ≥ 0.5. Using these automated criteria, 30 of the 258 earthquakes were selected as potential generators of infrasound (Figure 1 and Table 1).

Table 1. List of earthquakes selected based on the criteria explained in the text

Earthquake	Date	Event Time, UT	Location	M_L	Latitude, (°)	Longitude(°)	Depth (km)
1	18-Aug-2007	13:14:25	Northwest Arizona	3.11	36.4682	-110.328	7.68
2	18-Jan-2008	23:06:30	Valley of fire, Nevada	3.05	36.4985	-114.516	3.66
3	21-Feb-2008	14:16:02	Wells, Nevada	5.91	41.1332	-114.862	7.6
4	21-Feb-2008	14:34:41	Wells, Nevada	4.51	41.1495	-114.868	5.7
5	21-Feb-2008	18:55:52	Wells, Nevada	3.02	41.158	-114.827	7.85
6	21-Feb-2008	22:17:19	Wells, Nevada	3.21	41.1547	-114.877	6.7
7	22-Feb-2008	1:50:05	Wells, Nevada	4.03	41.1282	-114.874	8.08
8	22-Feb-2008	23:24:03	Wells, Nevada	3.55	41.1078	-114.915	7.88
9	22-Feb-2008	23:27:45	Wells, Nevada	4.48	41.1055	-114.9	7.35
10	27-Feb-2008	7:59:37	Wells, Nevada	4.47	41.2033	-114.851	6.35
11	29-Feb-2008	7:19:11	Wells, Nevada	3.27	41.2008	-114.86	5.55
12	1-Apr-2008	13:16:17	Wells, Nevada	4.54	41.2257	-114.844	9.02
13	22-Apr-2008	20:40:08	Wells, Nevada	4.32	41.2237	-114.845	4.94
14	23-Apr-2008	8:53:58	Montrose, Colorado	3.02	38.5537	-107.83	8.37
15	2-Oct-2008	22:55:09	Caliente, Nevada	3.31	37.3542	-114.548	1.7
16	16-Jan-2009	4:15:34	Alpine, Wyoming	4.08	43.2138	-111.013	1.35
17	19-Jan-2010	3:39:39	Yellowstone Natl. Park	3.33	44.5635	-110.968	6.22
18	12-Feb-2010	22:37:09	Kanab, Utah	3.02	37.0918	-112.892	11.89
19	5-Aug-2010	14:59:27	Jackson, Wyoming	4.31	43.5978	-110.414	0.09
20	7-Sep-2010	10:08:26	Island Park, Montana	3.39	44.9513	-111.739	3.3
21	26-Oct-2010	4:12:46	Jackson, Wyoming	3.34	43.6008	-110.396	0.53
22	6-Nov-2010	20:39:05	Kanab, Utah	3.05	37.0103	-112.879	11.19
23	15-Dec-2010	21:59:57	Alpine, Wyoming	3.29	43.0692	-110.8	0.82
24	26-Dec-2010	15:53:54	Lima, Montana	3.05	44.7363	-111.735	7.67
25	3-Jan-2011	12:06:36	Circleville, Utah	4.56	38.2473	-112.34	5.4
26	3-Jan-2011	20:23:45	Circleville, Utah	3.24	38.2378	-112.338	1.83
27	6-Jan-2011	22:31:04	Circleville, Utah	3.46	38.2622	-112.334	2.92
28	12-Jan-2011	8:46:29	Circleville, Utah	3.58	38.2385	-112.341	4.73
29	20-Jan-2011	21:59:12	Fayette, Utah	3.25	39.1622	-111.909	9.86
30	26-Jan-2011	5:10:11	Montpelier, Idaho	3.73	42.424	-111.499	5.76

Characteristics of the detections are summarized in Figure 2. The magnitudes analyzed are primarily $M_L < 4.5$ and the recorded distances < 250 km. Somewhat unusual are the short durations measured in this analysis when compared to Mutschlecner and Whitaker (2005), Figure 3. It is important to note that there are differences in our measurement techniques and those of previous authors. In this analysis, we utilize the duration of the detection as determined by InfraMonitor. This is a function of the window length, overlap, and p-value applied in the detector. Mutschlecner and Whitaker (2005) used inspection of the correlation, azimuthal deviation, and group velocity to measuring duration. Also, Mutschlecner and Whitaker (2005) focused primarily on stratospheric returns. Many of our measurements have group velocities > 300 m/s and are probably better associated with ducted tropospheric arrivals. The two datasets are clearly different. While measurement differences are one possible explanation, the two datasets also have little overlap in magnitude. These differences will be a focus of continued research. A first next step will be the analysis of distance and path corrections for the measured amplitudes.

Observations from the January 3, 2011, Circleville Earthquake

An earthquake with M_L 4.6 (M_w 4.6) occurred on January 3, 2011, at 12:06:37 UTC, within a known seismically active belt along the western side of the Sevier Valley in the Tushar Mountains (in the proximity of the city Circleville, UT) (Figure 1). The event was widely felt in the surrounding communities and had a normal faulting mechanism and a depth constrained, by full moment tensor calculation, between 5 and 9 km. The main shock and 85 aftershocks were recorded by Utah's regional seismic network. Epicentral infrasound from the main event was detected on six of the nine infrasonic arrays distributed across the state of Utah (Figure 4). Possible scattered infrasound was found at some of the other arrays. The event and associated data allow us to explore (as part of an on-going project) possible models of infrasound generation from earthquakes based on models of earthquake source ground motion parameters (acceleration, velocity).

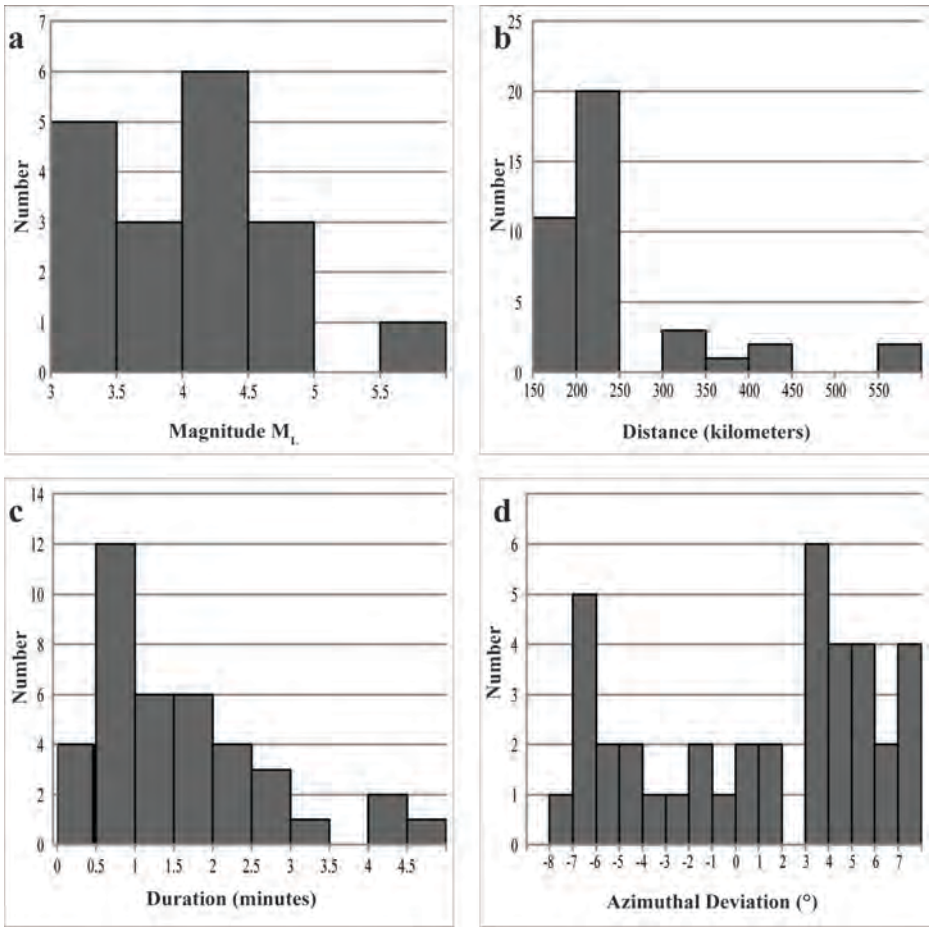

Figure 2. Histograms showing the distribution of detection characteristics for the first detection list (red symbols, Figure 1): (a) magnitude range of earthquakes with detections (N = 18), (b) Distance range of detections (N = 39), (c) range in duration of infrasound signals (N = 39), and (d) range in azimuthal deviation with respect to epicenter determined from seismic data (N = 39).

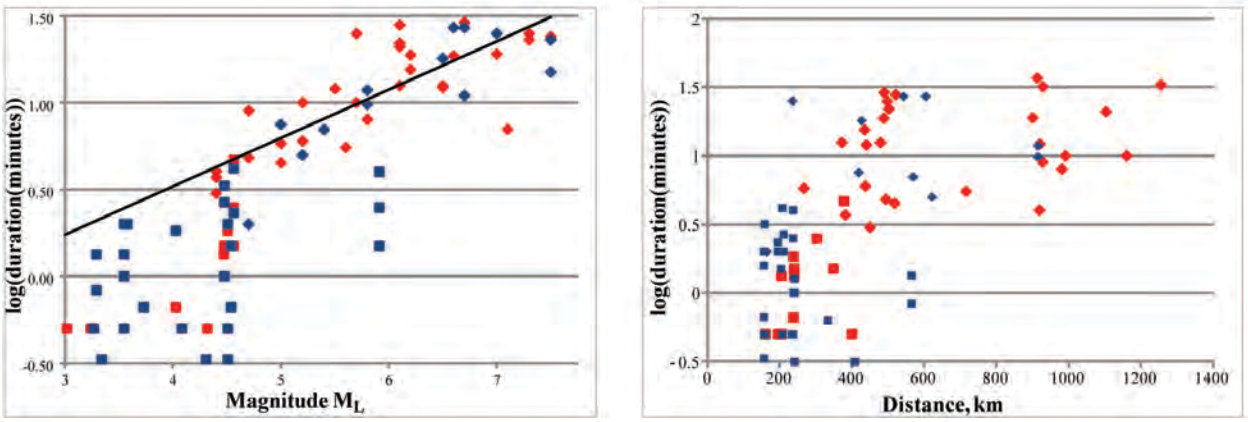

Figure 3. Log duration measurements versus magnitude (M_L) and distance for the detections found in this study (squares) and those determined by Mutschlecner and Whitaker, 2005 (diamonds). Red symbols are for stratospheric returns (group velocities between 280 and 310 m/s, Ceplecha et al., 1998). The black line in the left-hand panel is the scaling relation determined by Mutschlecner and Whitaker (2005) with M_L.

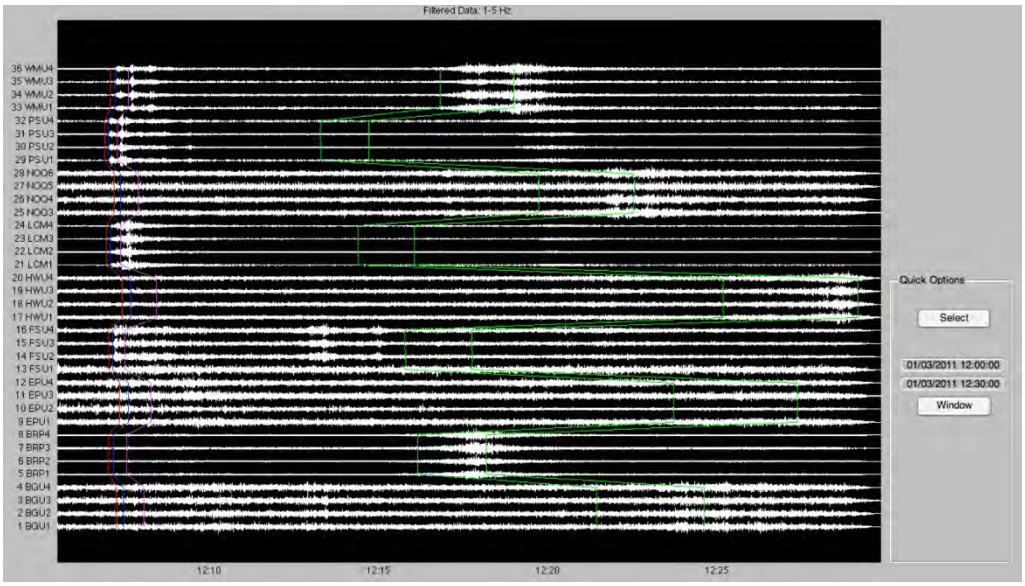

Figure 4. Infrasound signals filtered in the 1–5 Hz band. The colored lines represent the expected times for seismic phases (red, blue, and purple) and for epicentral infrasonic arrivals (green) with group velocities between 0.22 and 0.35 km/s.

Based on these observations, the source of the infrasound signals was located (Figure 5). The location solution for the infrasound source was estimated using the Bayesian infrasonic source location (BISL, Modrak et al., 2010) method. Six arrays (yellow triangles) were used for the final solution. Epicentral infrasound was not detected at the other three arrays (red triangles). The 75, 90, and 95 percent credibility contours are shown. The seismic epicenter is the red star. It is clear that these infrasound signals were generated within the epicentral region and may be one of the first documented observations of epicentral infrasound from a small earthquake. A preliminary search for infrasound associated with the aftershocks has produced possible single array detections for three of the larger aftershocks.

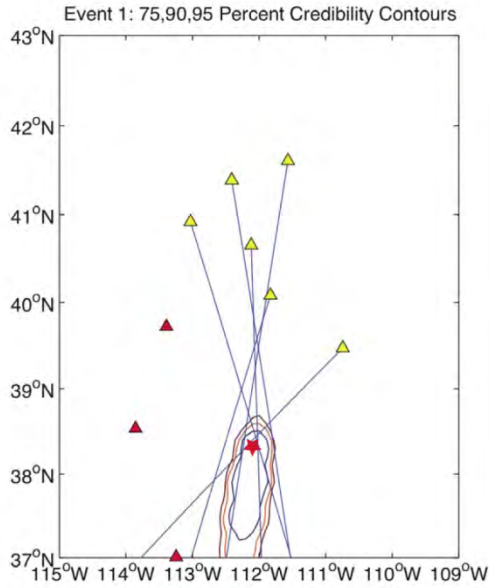

Figure 5. Location solution of epicentral infrasound estimated using the BISL method (Modrak et al., 2010). Six arrays (yellow triangles) were used in the final solution. Epicentral infrasound was not detected at the other three arrays (red triangles). The 75, 90, and 95 percent location credibility contours are shown. The seismic location is represented by the red star.

Three of the infrasound arrays (solid red triangles in Figure 5) produced no associated infrasound signals. A modeling exercise using both the parabolic equation (PE) and ray tracing was undertaken to quantify the path effects. The G2S atmospheric model of Drob et al. (2010) was used in these simulations, taking into account atmospheric effects at the specific time of the observations. The PE solutions are reproduced in Figure 6. These simulations indicate that the paths to LCMT, PSUT, and FSU (Figures 1 and 5) are not expected to produce arrivals under the atmospheric conditions at the time of the earthquake, consistent with the observations. Stations to the north and east of the source lie either within or close to predicted paths from G2S. These results illustrate the importance of the inclusion of time-dependent atmospheric effects and modeling in order to interpret the infrasound data. Further, these results suggest that the lack of an infrasound arrival from an earthquake at a specific array cannot be used to conclude that infrasound was not generated by the event.

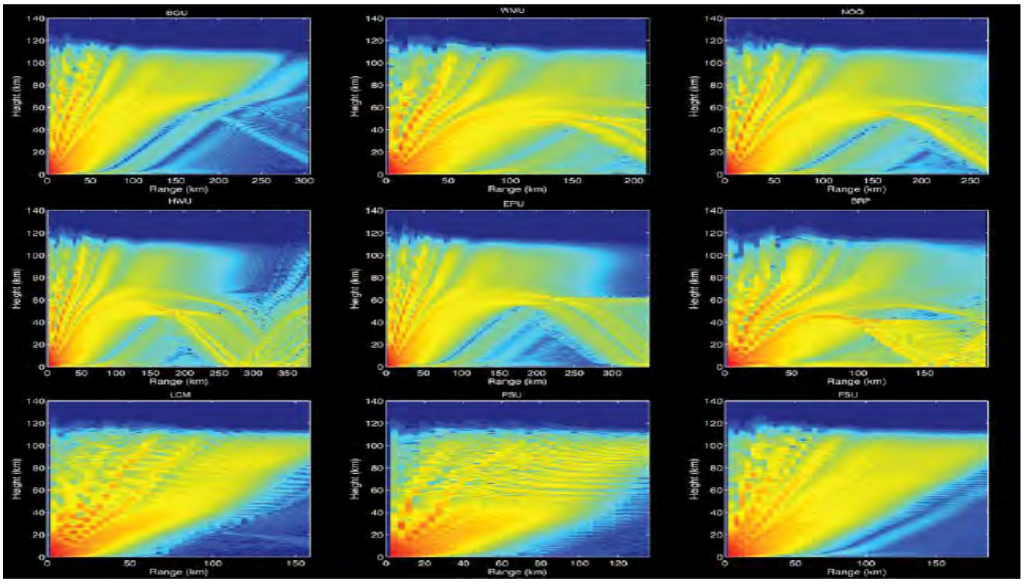

Figure 6. PE simulations for all nine UU infrasound arrays for the main event. The top two rows show simulations for the six arrays that detected the earthquake (yellow triangles in Figure 5), while the bottom row shows simulations for three arrays that did not detect the earthquake (red triangles in Figure 5).

Modeling the January 3, 2011, Circleville earthquake

A hybrid procedure for modeling infrasound signals generated by earthquakes is under development and has been tested using data from the Circleville earthquake and is similar to work reported by Arrowsmith et al. (2011) also in this volume. The procedure is broken into four distinct steps, each of which is illustrated for this event: (1) constraint of peak near-source accelerations based on the ShakeMap (Wald et al., 2003) solution for the event, (2) generation of synthetic acceleration time histories on a 2D grid in the epicenter region, (3) modeling of the near-field acoustic pressure waveform using the Rayleigh Integral, and (4) generation of the acoustic waveform at the receiver using time domain parabolic equation modeling.

The ShakeMap solution for the peak horizontal acceleration for the Circleville earthquake is reproduced in Figure 7. This solution consists of predicted free surface maximum ground motions as a function of location based on empirical ground motion prediction equations for small earthquakes (Wald et al., 2003) combined with empirical site amplification terms based on the local surface geology (Borcherdt, 1994).

A 3D finite difference technique (Larson and Schultz, 1995) is used to compute the acceleration time histories on a 2D grid over a 40 × 40 km^2 region directly above the hypocenter. The solution relies on a Gaussian source time function in velocity, a 1D velocity model that UUSS uses for earthquake location in the region, and the source depth and moment tensor from the Harvard centroid moment tensor (CMT) catalog. These waveforms are subsequently scaled by the ShakeMap solution to provide consistent absolute amplitudes above the hypocenter.

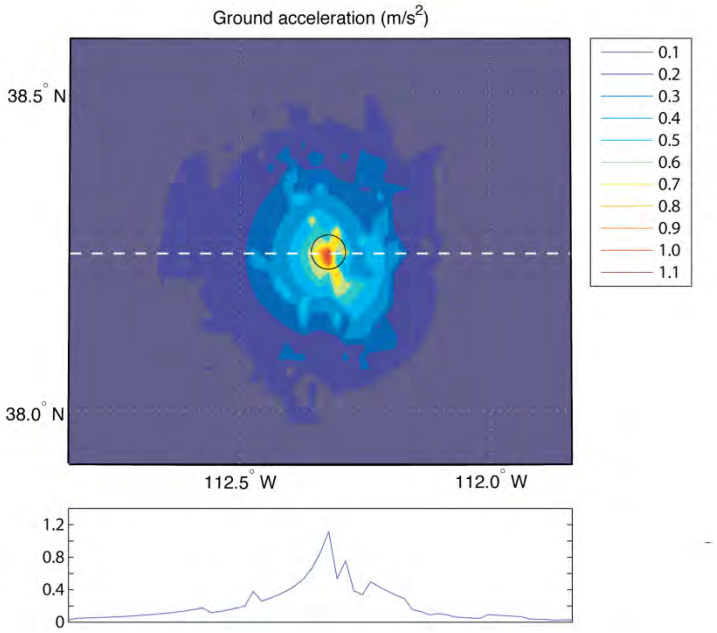

Figure 7. ShakeMap contours of ground acceleration in m/s^2 (the black circle denotes a circle of radius 3 km, used for the Rayleigh integral calculation). The bottom panel shows a profile along the white dashed line (y-axis is acceleration).

The pressure time history in the atmosphere directly above the epicenter is computed using the Rayleigh integral (Blackstock, 2000), which gives the pressure at some distance from a baffled piston (i.e., all radiation is restricted to the forward direction) and integrates contributions from accelerations of all infinitesimal area elements, *dS*, of the piston in the epicentral region. Based on numerical tests, the first ~10 s can be adequately modeled using the Rayleigh integral because the surface area of ground accelerations is small enough that the far-field assumption inherent in the Rayleigh integral is valid. Beyond 10 s, the assumption that all the energy comes from the 3 × 3 km surface area is not valid. Thus, the Rayleigh integral is suitable for modeling the initial ground pumping from the earthquake. The procedure is a modification of that used by Green et al. (2009) to model ground-to-air coupling of the 2007 Folkestone earthquake in the United Kingdom, although their simulations relied on topographic coupling displaced from the epicenter. The Rayleigh integral is expressed as

$$p(x, y, z; t) = \rho_0 \int_s \frac{\dot{u}_p(x', y'; t - R/c_0)}{2\pi R} dS$$

where *x'*, *y'* are the coordinates of the source point on the piston, *R* is the distance to the field point of interest, ρ_0 is the air density, and c_0 is the speed of sound in air.

The pressure *on-axis* at an elevation of 5 km is calculated using the acceleration-time histories from the 3D finite difference modeling due to a 3 × 3 km^2 region. The resulting pressure time history, with a peak of ~300 Pa, is shown in Figure 8.

The radiation pattern as a function of take-off angle can be characterized by an amplitude directivity factor D, which is defined as the pressure at any angle θ relative to that (at the same range r) at θ = 0:

$$D(\theta) = \frac{P(r,\theta)}{P(r,0)}.$$

The radiation pattern from a circular piston with radius of *a* is calculated from (Blackstock, 2000):

$$D(\theta) = \frac{2J_1(ka\sin\theta)}{ka\sin\theta}$$

where J_1 is the first-order Bessel function of the first kind, k is the wavenumber ($k = 2\pi/\lambda$), and θ is the angle from the zenith. The number of nulls and secondary maxima in the radiation pattern is determined by the size of ka. As the piston size increases, relative to the wavelength, the number of nulls increases.

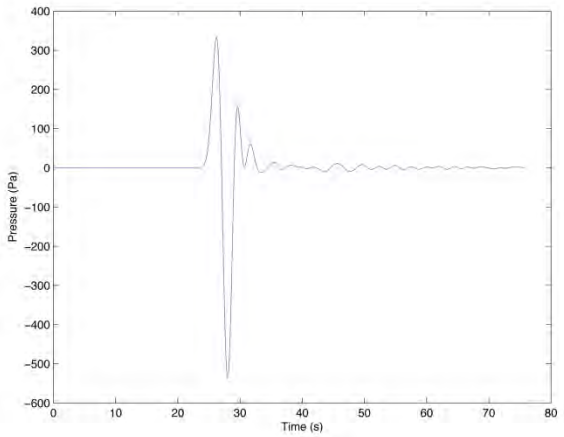

Figure 8. Predicted pressure waveform at 5 km above the peak ground acceleration from the Circleville earthquake epicenter.

In order to compute the far-field acoustic signals and compare with the observations, we used a time-domain PE that incorporates gravity waves. The starting waveform is the predicted near-field acoustic pressure (Figure 8) scaled by a factor of 200 to account for directivity effects. The computed waveforms are compared to the observations in Figure 9. We note that the peak-to-peak amplitudes are robust for different gravity wave realizations, although other characteristics of the waveforms can vary (such as energy from weak ducts). The synthetics compare well with the observations from the six observing arrays. Both the peak amplitudes and the arrival times in the synthetics are in agreement with the observations. At several of the stations the synthetics also have extended durations similar to the data. These comparisons suggest that the “baffled piston” model can explain infrasound observations from this earthquake.

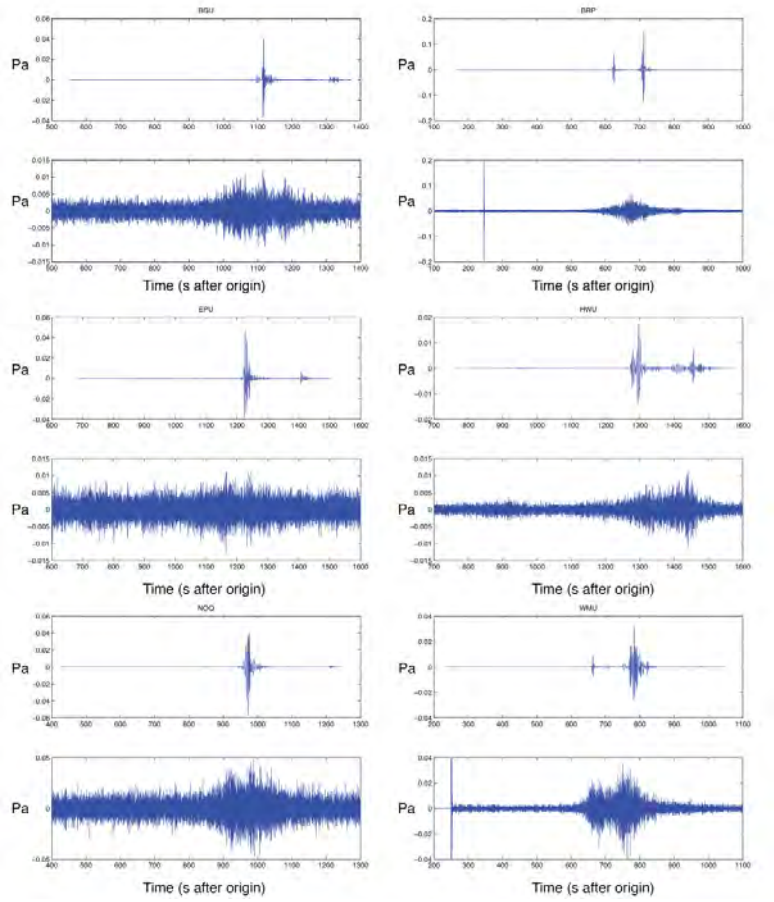

Figure 9. An absolute comparison of the modeled infrasound waveforms (top figure in each pair) with the six observations (bottom figure in each pair) for the Circleville, UT, earthquake. The peak amplitudes, arrival times, and signal durations are all well matched.

CONCLUSIONS AND RECOMMENDATIONS

A network of nine infrasound arrays had been co-located with existing seismic stations that are part of UUSS and are being operated in near real time. Time series from these stations are beginning to provide a dataset for automated signal detection and association and location of events within the Intermountain Seismic Belt. This region produces many moderate-sized earthquakes and is a source of active near-surface and underground mining, as well as a region with military activity that can generate acoustic signals. Initial results have been presented summarizing possible earthquakes that may have generated infrasound. Although the number of possible sources is modest, these results suggest that infrasound may accompany moderate-sized earthquakes.

On January 3, 2011, an M_w 4.6 earthquake occurred near Circleville, Utah, at an estimated depth between 5 and 9 km. Robust infrasound signals were detected at six of the nine infrasound arrays surrounding the event. These observations were used with the BISL methodology to estimate the source of the infrasound signals. The resulting uncertainty analysis includes the seismic epicenter location and suggests that the observed signals were so-called epicentral infrasound. PE and ray tracing modeling were undertaken to explain the lack of observations at the remaining stations. Using the G2S atmospheric model for the time of the earthquake, the stations that did not have observations were predicted to have no arrivals. The remaining six stations were either within or near regions where the models predicted arrivals. These simulations and the dataset illustrate the possible utility of the G2S model in interpreting observational data at these ranges.

A hybrid modeling procedure to predict infrasound waveforms from earthquakes was applied to the Circleville earthquake for comparison to the observations. The model relies on the constraint of peak ground acceleration using ShakeMap. A 2D grid of ground motion time histories directly above the source are estimated using a 3D simulation constrained by local geological models and the estimated source function and scaled to the ShakeMap results for the earthquake. The resulting scaled acceleration time histories are input into the Rayleigh integral to estimate the acoustic pressure time history directly above the epicenter. A time domain PE that incorporates gravity waves is then used to propagate the acoustic signal to regional distances. The predicted regional signals were consistent with the amplitude, arrival time, and duration of observations made at the six stations. These preliminary results suggest that the signals were from the earthquake epicenter and support the "baffled piston" model for the generation of infrasound from earthquakes.

Future work will include the continued operation of the network, archival of the data at the IRIS DMC, automated processing of the data with the development of event bulletins and the interpretation of the resulting events. The hybrid earthquake epicenter model for regional infrasound will be further assessed with additional earthquake observations. Our objective is to develop a physical understanding of the types of earthquake parameters that can lead to the generation of infrasound. This information, along with the physical understanding of the generation and propagation of infrasound from near-surface explosions, will be used to assess the utility of combined seismic and infrasound discriminants.

REFERENCES

Arrowsmith, S. J., R. Whitaker, and R. Stead (2011). Infrasound as a depth discriminant, these Proceedings.

Arrowsmith, S. J., R. Whitaker, S. R. Taylor, R. Burlacu, B. Stump, M. Hedlin, G. Randall, C. Hayward, and D. ReVelle, (2008). Regional monitoring of infrasound events using multiple arrays: Application to Utah and Washington State, *Geophys. J. Int.* 175:1, 291–300.

Blackstock, D. T. (2000). *Fundamentals of Physical Acoustics*, Wiley-Interscience, New York.

Borcherdt, R. D. (1994). Estimates of site-dependent response spectra for design (methodology and justification), *Earthquake Spectra* 10: 617 – 653.

Burlacu, R., S. Arrowsmith, K. L. Pankow, M. J. Hale, C. Hayward, and B. W. Stump (2010). A network of infrasonic arrays in Utah, 2010 Fall Meeting, AGU, San Francisco, California, 13–17 December.

Ceplecha, Z., J. Borovicka, W. G. Elford, D. O. ReVelle, R. L. Hawkes, V. Porubcan, and M. Simek (1998). Meteor phenomena and bodies, *Space Sci. Rev.* 84: 327–471.

Che, I-Y., M-S Jun, J-S Jeon, and K Min (2002). Analysis of seismo-acoustic events in the Korean Peninsula. *Geophys. Res. Lett.* 29:12.

Drob, D. P., M. Garces, M. A. H. Hedlin, and N. Brachet (2010). The temporal morphology of infrasound propagation, *Pure Appl. Geophys.*, doi:10.1007/s00024-010-0080-6.

Green, D. N., J. Guilbert, A. Le Pichon, O. Sebe and D. Bowers (2009). Modeling ground-to-air coupling for the shallow M_L 4.3 Folkestone, United Kingdom, Earthquake of 28 April 2007, *Bull. Seism. Soc. Am.* 99:4, 2541–2551, doi: 10.1785/0120080236.

Hale, J., S. Arrowsmith, C. Hayward, R. Burlacu, K. Pankow, B. Stump, G. Randall, and S. Taylor (2010). Infrasound signal characteristics from small explosions, *Proceedings of the 2010 Monitoring Research Review: Ground-Based Nuclear Explosion Monitoring Technologies*, LA-UR-10-05578, Vol. II. pp. 720–730.

Kim, T. S., C. Hayward, and B. Stump (2004). Local infrasound signals from the Tokachi-Oki earthquake, *Geophys. Res. Lett.* 31:20, L20605 10.1029/2004GL021178.

Larsen, S. and C. A. Schultz (1995). ELAS3D: 2D/3D elastic finite-difference wave propagation code, Lawrence Livermore National Laboratory technical report UCRL-MA-121792.

Le Pichon, A., P. Mialle, J. Guilbert, and J. Vergoz (2006). Multistation infrasonic observations of the Chilean earthquake of 2005 June 13, *Geophys. J. Int.* 167: 838–844.

Modrak, R. T., S. J. Arrowsmith, and D. N. Anderson (2010). A Bayesian framework for infrasound location, *Geophys. J. Int.* 181:399–405.

McKenna, M. H., B. W. Stump, S. Hayek, J. R. McKenna, and T. R. Stanton (2007). Tele-infrasonic studies of hard-rock mining explosions, *J. Acoust. Soc. Am.* 122: 97–106.

Mutschlecner, J. P. and R. W. Whitaker (2005). Infrasound from earthquakes, *J. Geophys. Res.*, 110:D01108, doi:10.1029/2004JD0050067.

Smith, R. B. and W. J. Arabasz (1991). Seismicity of the Intermountain Seismic Belt, in *Neotectonics of North America*, Slemmons, D. B., Engdahl, E. R., Zoback, M. L., Blackwell, and D. D., Eds., Geological Society of America, Boulder, CO, pp. 185–228.

Sorrells, G. G., E. Herrin, and J. L. Bonner (1997). Construction of regional ground-truth data base, *Seismo. Res. Lett.* 68: 743–752.

Wald, D. J., B. C. Worden, V. Quitoriano, and K. L. Pankow (2003). *ShakeMap Manual: Technical Manual User's Guide and Software Guide*, U.S. Geological Survey Techniques and Methods, book 12, section A, Chap 1.